

## The CRESST dark matter search - Status and Perspectives

---

F. Reindl<sup>\*a</sup>, G. Angloher<sup>a</sup>, A. Bento<sup>b</sup>, C. Bucci<sup>c</sup>, L. Canonica<sup>c</sup>, X. Defay<sup>d</sup>, A. Erb<sup>d e</sup>, F. v. Feilitzsch<sup>d</sup>, N. Ferreiro Iachellini<sup>a</sup>, P. Gorla<sup>c</sup>, A. Gütlein<sup>f</sup>, D. Hauff<sup>a</sup>, J. Jochum<sup>g</sup>, M. Kiefer<sup>a</sup>, H. Kluck<sup>f</sup>, H. Kraus<sup>h</sup>, J.-C. Lanfranchi<sup>d</sup>, J. Loebell<sup>g</sup>, A. Münster<sup>d</sup>, C. Pagliarone<sup>c</sup>, F. Petricca<sup>a</sup>, W. Potzel<sup>d</sup>, F. Pröbst<sup>a</sup>, K. Schöffner<sup>c</sup>, J. Schieck<sup>f</sup>, S. Schönert<sup>d</sup>, W. Seidel<sup>a</sup>, L. Stodolsky<sup>a</sup>, C. Strandhagen<sup>g</sup>, R. Strauss<sup>a</sup>, A. Tanzke<sup>a</sup>, H.H. Trinh Thi<sup>d</sup>, C. Türkoğlu<sup>f</sup>, M. Uffinger<sup>g</sup>, A. Ulrich<sup>d</sup>, I. Usherov<sup>g</sup>, M. Wüstrich<sup>a</sup>, S. Wawoczny<sup>d</sup>, M. Willers<sup>d</sup>, A. Zöller<sup>d</sup>

E-mail: [florian.reindl@mpp.mpg.de](mailto:florian.reindl@mpp.mpg.de)

<sup>a</sup>Max-Planck-Institut für Physik, D-80805 München, Germany

<sup>b</sup>Departamento de Fisica, Universidade de Coimbra, P3004 516 Coimbra, Portugal

<sup>c</sup>INFN, Laboratori Nazionali del Gran Sasso, I-67010 Assergi, Italy

<sup>d</sup>Physik-Department and Excellence Cluster Universe, Technische Universität München, D-85747 Garching, Germany

<sup>e</sup>Walther-Meißner-Institut für Tieftemperaturforschung, D-85748 Garching, Germany

<sup>f</sup>Institut für Hochenergiephysik der Österreichischen Akademie der Wissenschaften, A-1050 Wien, Austria and Atominstytut, Vienna University of Technology, A-1020 Wien, Austria

<sup>g</sup>Eberhard-Karls-Universität Tübingen, D-72076 Tübingen, Germany

<sup>h</sup>Department of Physics, University of Oxford, Oxford OX1 3RH, United Kingdom

In August 2015 the direct dark matter search CRESST-II finished its second extensive data taking campaign (phase 2), after more than two years of measurement time. We present a preliminary analysis of a small data set of a single detector module called Lise. This detector features a threshold of 0.3 keV which is the lowest value for all detectors operated in phase 2. We show that the performance of this detector allows to efficiently make use of the low detection threshold providing high potential for a substantial gain in sensitivity in the regime of low dark matter particle masses.

*The European Physical Society Conference on High Energy Physics  
22-29 July 2015  
Vienna, Austria*

---

\*Speaker.

## 1. Introduction

In the recent years low mass dark matter particles gained interest, from theoretical as well as from experimental side. Since such particles ( $\mathcal{O}(< 10 \text{ GeV}/c^2)$ ) transfer only tiny energies in a scattering process a low energy threshold is crucial for the sensitivity of an experiment in the low mass regime. CRESST-II is a direct dark matter search, located in the Gran Sasso underground lab (LNGS) in central Italy. Two signals are recorded simultaneously for every particle interaction in the  $\text{CaWO}_4$  target crystals: the phonon (heat) signal providing a precise measurement of the deposited energy, independent of the type of particle. The light signal measuring the scintillation light emitted by the crystal is used to identify the type of particle - a powerful tool to discriminate backgrounds. Both channels use thermometers made of thin tungsten films, so-called transition edge sensors (TESs), either directly attached to the crystal in case of the phonon channel or evaporated onto a light absorber in case of the light channel.

CRESST-II finished its second phase in August 2015, which was started in July 2013. In 2014 we analyzed the first data from phase 2 which were taken in 2013 [1]. With this non-blind analysis of a single upgraded detector module we explored new parameter space for WIMP masses below  $3 \text{ GeV}/c^2$ . While all detectors in previous measurements [2] and the majority of detectors in the current phase hold the crystal with bare metal clamps, the upgraded design uses  $\text{CaWO}_4$ -sticks instead. The benefit of these sticks is that there is no line-of-sight between the crystal and non-active (non-scintillating) surfaces which eliminates any background events related to  $\alpha$ -decays of, in particular,  $^{210}\text{Po}$ . Additionally, the detector module analyzed in [1] is equipped with a  $\text{CaWO}_4$  crystal grown by the Technische Universität München. It exhibits a considerably lower  $e^-/\gamma$ -background level compared to the commercial crystals used for most other modules. These features, combined with an energy resolution of  $\sigma \simeq 100 \text{ eV}$  and an energy threshold of  $0.6 \text{ keV}$ , clearly result in a superior overall performance compared to all other modules operated in the current phase.

With this analysis we proved for the first time that CRESST-II detectors are sensitive to recoil energies below  $1 \text{ keV}$ . Based on this finding we optimized the trigger settings of all detectors with a comparable phonon performance to the lowest threshold setting still allowing a stable long-term operation. Baseline noise and achievable threshold are connected: As a rule of thumb, stable operation is possible with a threshold value of five times the baseline noise. In this contribution we present a preliminary analysis of the detector called Lise which provides the best energy resolution ( $\sim 60 \text{ eV}$ ) and, therefore, the lowest trigger threshold of  $0.3 \text{ keV}$ .

## 2. New Data

We perform a blind analysis defining a statistically insignificant part of the data as the so-called training set. All methods of data selection are developed on this set and then applied without change - blindly - to the remaining data. In this contribution we present a preliminary analysis from the training set. Figure 1 presents the resulting data in the light yield-energy plane. The light yield is defined as the ratio of energy measured in the light channel divided by the energy measured in the phonon channel. The dominant background is  $e^-/\gamma$ -events (recoils on electrons) originating from intrinsic contaminations of the crystal. These events have a light yield normalized to one.<sup>1</sup>

<sup>1</sup>In a strict sense they have a light yield of one at  $122 \text{ keV}$ , the energy of the  $^{57}\text{Co}$   $\gamma$ -source used for calibration.

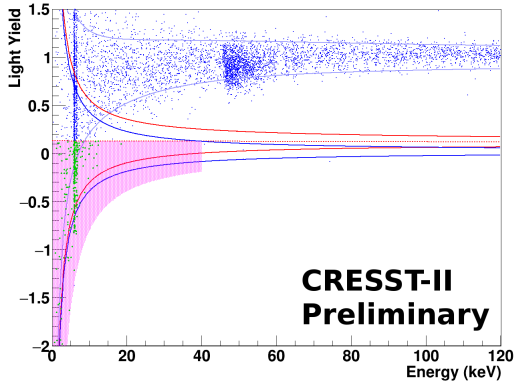


**Figure 1:** Data of the training set of the detector module Lise. Different event classes exhibit different light outputs. The solid lines depict the boundaries with 80 % of the corresponding events expected in between, light-blue for electron recoils, red for recoils off oxygen and blue for those off tungsten. The upper boundary of the acceptance region for the dark matter search (shaded red) is set to the mean of the oxygen band (dashed red). Events inside the acceptance region are highlighted in green.

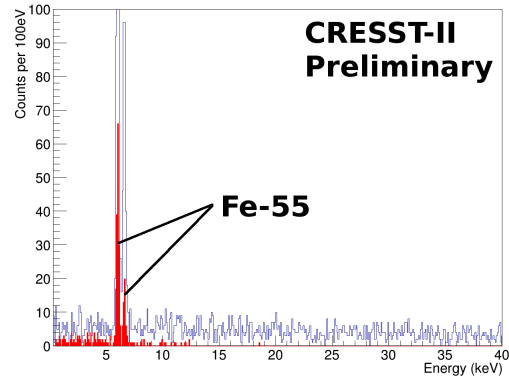


**Figure 2:** Energy spectrum of all events (blue) and events in the acceptance region (red). Both spectra are flat down to the energy threshold of 0.3 keV.

By a fit of the data we extract the mean of the  $e^-/\gamma$ -band and the width, both as a function of energy. The width of the band is dominated by the resolution of the light detector, in particular for this module as it combines a highly-performing phonon detector with a light detector of modest performance. The result of this fit is drawn in the light-blue lines marking the upper and lower 90 % boundaries of the  $e^-/\gamma$ -band. Thus, 80 % of electron recoil events are expected between those two lines.

Nuclear recoils exhibit a lower light output than electron recoils quantified by so-called quenching factors precisely determined in dedicated experiments [3]. With this quenching factors we then calculate the nuclear recoil bands, oxygen in solid red, tungsten in solid blue (calcium not drawn). Analogues to [1] we accept any nuclear recoil event below the mean of the oxygen band (dashed red) and above the 99.5 % lower boundary of the tungsten band as a potential scattering of a dark matter particle. The accepted energy range extends from the threshold up to 40 keV. The resulting region is shaded in red, with the events therein highlighted in green.

Two features in the background spectrum depicted in figure 2 are evident, first a  $\beta$ -spectrum at 46 keV originating from a  $^{210}\text{Pb}$  contamination of the crystal. In the current phase we equipped some light detectors with an  $^{55}\text{Fe}$ -source to allow for an absolute calibration of the light channel. One of those sources, installed for the calibration the light detector of a near-by module, accidentally illuminated the module Lise causing the double line at around 6 keV. However, the low dark matter particles masses investigated in this contribution are expected to induce recoils of much lower energy only. Thus, the  $^{55}\text{Fe}$  double-peak has hardly any impact on the final result.

### 3. Trigger and Cut Efficiency

For a low threshold analysis the precise knowledge of the trigger threshold and the cut efficiency is crucial. We measure the trigger threshold by injecting small electrical pulses of variable particle-equivalent energy to the heater. For each injected energy we calculate the ratio of the number of pulses triggering and the number of pulses sent to the heater (see blue dots in figure 3). The finite baseline noise of the detector causes a broadening of the step-wise trigger threshold. Thus, we fit the data with the function  $\frac{1}{2}[(1 + \operatorname{erf}(\frac{x-\mu}{\sigma\sqrt{2}}))]$  which one obtains by convolving a step-function and a Gaussian function. The free parameters  $\mu$  and  $\sigma$  then correspond to the threshold energy and the baseline noise as seen by the trigger, respectively. We obtain values of  $\mu = 298\text{eV}$  and  $\sigma = 84\text{eV}$ . The value for  $\sigma$  is slightly worse than the one we obtain for the energy reconstruction ( $\sigma = 60\text{eV}$ ) of the particle pulses. This may be attributed to low frequency disturbances on the baseline which can be corrected by the off-line processing of the pulses but not by the trigger electronics.

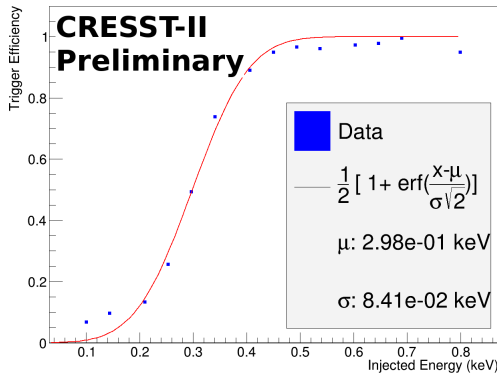


**Figure 3:** Measured trigger efficiency as a function of injected energy. The blue points depict the ratio between the number of pulses triggering to the total number of pulses sent. The fit function is drawn in red, the resulting parameters for  $\mu$  and  $\sigma$  are given in the legend.

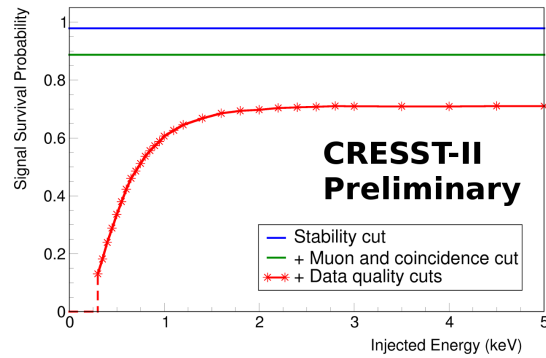


**Figure 4:** Cumulative cut efficiency, beginning with the cut on detector stability (blue). The green line refers to the efficiency after stability cut plus the removal of events coincident with the muon veto or another detector. After that, data quality cuts are applied, resulting in the final efficiency (red).

We randomly read out the detectors without a prior trigger signal. These so-called empty baselines we then superimpose with pulses corresponding to nuclear recoils of different energies. The result of this procedure is a data set of artificial pulses affected by artifacts, like e.g. a time-dependent noise level, in the same manner as events caused by particle interactions. By processing these artificial data just like *normal* data one can then extract the cut efficiency, the survival probability for potential signal events, drawn as a function of energy in figure 4. The first cut we apply is the stability cut removing time periods of unstable detector operation. Secondly, we remove all events coincident with any other detector or the muon veto. The tiny interaction probability expected for dark matter particles basically excludes interactions in more than one detector. Coincidences with the muon veto are discarded since muons might produce, among other particles, neutrons which induce nuclear recoils and therefore potentially mimic a dark matter signal. How-

ever, the vast majority of events removed by this cut are random coincidences causing a constant fraction of events to be removed. Since we extract the energy of an event from the height of the recorded pulse we allow for very small deviations from the nominal pulse shape only. The identification of pulses with a different shape gets more challenging for very small pulses which causes the pronounced energy dependence of the data quality cuts (red line in figure 4) below 3 keV.

#### 4. Energy Spectrum and Result

Figure 2 depicts the energy spectra of the events in the training set, in blue for all events, in red for events in the acceptance region. We find a rather flat background down to threshold energy, in particular when keeping in mind the decreasing cut efficiency. Clearly visible is the double peak from the  $^{55}\text{Fe}$ -source, which is also present in the acceptance region. This is a result of the below average performance of the light detector causing a poor discrimination between electron and nuclear recoil bands which can also be seen in figure 1.

We use Yellin's optimum interval [4] method to extract a limit (90% C.L.) on the cross-section of the scattering of dark matter particles with nucleons as a function of their mass. Basically, this method exploits the differences between the measured and the expected spectrum<sup>2</sup> to set an upper limit on the cross-section. We do not apply any background subtraction, all events in the acceptance region are conservatively considered as potential dark matter events. However, we want to note that this approach might be too conservative as we know that the dominating background is leakage from the  $e^-/\gamma$ -band and, in addition, the Yellin method makes no use of the light yield information.

Several features of this limit deserve to be mentioned. Obviously, it is not competitive above masses of a few  $\text{GeV}/c^2$ , firstly because of the tiny exposure and secondly due to the enormous background level in the acceptance region. However, for masses below  $2\text{GeV}/c^2$  this result explores new parameter space, previously not covered by any other dark matter search experiment. The huge gain in sensitivity compared to the result of 2014 is mainly driven by a two times lower trigger threshold (0.6 keV to 0.3 keV). Additionally, this detector exhibits an almost flat background down to the trigger threshold.

The main design difference between Lise and the module for the 2014 limit is the different holding concept of the crystal; metal clamps vs.  $\text{CaWO}_4$ -sticks. However, we want to emphasize that all beneficial properties of Lise allowing for an improvement in the low mass regime are not connected to the holding. On the other side, for higher masses or in case a positive signal is observed, fully-active detector designs capable to veto  $^{210}\text{Po}$ -induced backgrounds are absolutely mandatory. Thus, for the future only fully-active designs will be used.

#### 5. Conclusion and Outlook

In this contribution we present a non-blind analysis of a very small data set obtained with the detector Lise, which is the one with the lowest trigger threshold among all detectors currently operated in CRESST-II. We have shown the high potential of this detector for a substantial gain of sensitivity in the regime of low dark matter particles masses, further improving our 2014 result.

<sup>2</sup>Calculated using standard assumptions on the dark matter halo and the form factor, as discussed e.g. in [1].

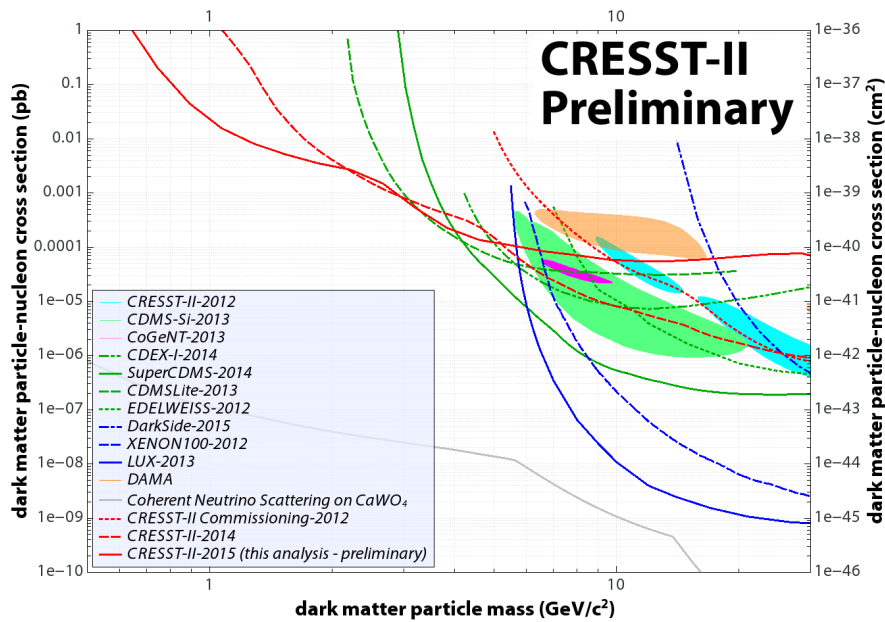


**Figure 5:** The direct detection landscape (as of July 2015) with 90% exclusion limits (lines, [1, 5, 6, 7, 8, 9, 10, 11, 12]) and regions compatible with excess signals (shaded areas, [2, 13, 14, 15]) as observed by various direct dark matter searches. Below the so-called neutrino-floor (depicted as gray line for  $\text{CaWO}_4$ , [16]) an experiment will be affected by the coherent neutrino-nucleus scattering. The preliminary result is drawn in solid red, exploring new parameter space below  $2 \text{ GeV}/c^2$ .

In September 2015<sup>3</sup> we presented the final blind analysis of the low-threshold data set for the detector Lise [18], corresponding to an exposure of 52 kg days. The final exclusion limit is very similar to the preliminary result presented in this contribution, however a slight improvement is seen, mainly due to the much higher exposure.

The result presented here illustrates once more the need for highly-performing phonon detectors reaching very low thresholds to further push the sensitivity for light dark matter particles. Thus, we take this result as a further encouragement to pursue our strategy (outlined in [19]) aiming for a threshold of less than 100 eV in the upcoming phase of the CRESST dark matter search.

## Acknowledgments

We are grateful to LNGS for their generous support of CRESST, in particular to Marco Guetti for his constant assistance. This work was supported by the DFG cluster of excellence: Origin and Structure of the Universe, by the Helmholtz Alliance for Astroparticle Physics, and by the BMBF: Project 05A11WOC EURECA-XENON.

## References

- [1] CRESST Collaboration, G. Angloher *et al.*, Eur. Phys. J. C **74** (2014), arXiv:1407.3146.

<sup>3</sup>At the same time also CDMSlite presented new results in [17].

- [2] CRESST Collaboration, G. Angloher *et al.*, Eur. Phys. J. C **72** (2012), arXiv:1109.0702.
- [3] R. Strauss *et al.*, Eur. Phys. J. C **74** (2014), arXiv:1401.3332.
- [4] S. Yellin, Phys. Rev. D **66** (2002), arXiv:physics/0203002.
- [5] A. Brown, S. Henry, H. Kraus, and C. McCabe, Phys. Rev. D **85**, 021301 (2012), arXiv:1109.2589.
- [6] SuperCDMS Collaboration, R. Agnese *et al.*, Phys. Rev. Lett. **112**, 241302 (2014), arXiv:1402.7137.
- [7] SuperCDMS Collaboration, R. Agnese *et al.*, Phys. Rev. Lett. **112**, 041302 (2014), arXiv:1309.3259.
- [8] EDELWEISS Collaboration, E. Armengaud *et al.*, Phys. Rev. D **86**, 051701 (2012), arXiv:1207.1815.
- [9] CDEX Collaboration, Q. Yue *et al.*, Phys. Rev. D **90**, 091701 (2014), arXiv:1404.4946.
- [10] XENON100 Collaboration, E. Aprile *et al.*, Phys. Rev. Lett. **109**, 181301 (2012), arXiv:1207.5988.
- [11] LUX Collaboration, D. S. Akerib *et al.*, Phys. Rev. Lett. **112**, 091303 (2014), arXiv:1310.8214.
- [12] DarkSide Collaboration, P. Agnes *et al.*, Phys. Lett. B **743**, 456 (2015), arXiv:1410.0653.
- [13] CoGeNT Collaboration, C. E. Aalseth *et al.*, Phys. Rev. D **88**, 012002 (2013), arXiv:1208.5737.
- [14] CDMS Collaboration, R. Agnese *et al.*, Phys. Rev. Lett. **111**, 251301 (2013), arXiv:1304.4279.
- [15] C. Savage, G. Gelmini, P. Gondolo, and K. Freese, Journal of Cosmology and Astroparticle Physics **2009**, 010 (2009), arXiv: 0808.3607.
- [16] A. Gütlein *et al.*, Astropart. Phys. **69**, 44 (2015), arXiv: 1408.2357.
- [17] SuperCDMS Collaboration, R. Agnese *et al.*, (2015), arXiv: 1509.02448.
- [18] CRESST Collaboration, G. Angloher *et al.*, (2015), arXiv: 1509.01515.
- [19] CRESST Collaboration, G. Angloher *et al.*, (2015), arXiv: 1503.08065.